Supplementary Information

1-Samples and archaeological sites

Cova Bonica (Vallirana, Barcelona)

Cova Bonica is a cave located in the NE of the Iberian Peninsula, ~30 km north of Barcelona (41°22'10.29"N, 1°53'38.64"E) and 402 meters above mean sea level. The original morphology of the cave was modified by mining for sparry calcite and the cave sediments were partially destroyed by earthmoving and subsequent mushroom farming. The site consists of a principal chamber (SP) and two small chambers on the right side of SP, one next to the entrance (SP1) and the second in the internal area (SP2) (Fig. S1A-B).

The stratigraphic sequence of Cova Bonica is represented in the HG34 cross-section (Fig. S1C) and consists of mud sediments supporting varying amounts of speleothem, bedrock limestone clasts and archaeological remains. Layer IV_2 is overlying the bedrock and corresponds to the first Holocene deposition in this area; it consists of clay and silt sediment supporting limestone and speleothem clasts. Layer IV_2 yielded numerous fragments of Early Neolithic pottery, lithic artifacts of rock crystal and jasper, a bone awl made from an ovicaprine metapodial, body ornaments, faunal and human remains, and abundant charcoal (Fig. S1E-I). The upper canine subjected to whole-genome analysis (Fig. S1D), labelled CB13 (CB13-HH34-IV_2-2407), was obtained from this layer in August 2013 and yielded a direct radiocarbon age of 6,410±30 years BP (Table S1) from Beta Analytic, Miami, (Beta-384724). A second Cova Bonica tooth sample, labelled CB14 (CB14-HH34-IV_2-3155), was excavated in 2014 from the same stratigraphic layer and has no direct radiocarbon date.

Layer XIX_2 overlies this Early Neolithic unit and consists of dark plastic mud sediments supporting limestone clasts. This layer contains abundant charcoal, scant Late Neolithic pottery and faunal remains and has been dated on a femur of *Ovis aries* to 4,215±30 years BP from ORAU laboratory in Oxford (OxA-30387). The uppermost unit of the stratigraphic sequence (layer 0) is formed of mixed sediments reworked by mining and mushroom farming and contains prehistoric, Iberian-Roman, and Medieval-Modern ceramics as well as scattered Cardial remains.

Galeria da Cisterna (Almonda karst system, Torres Novas, Portugal)

Galeria da Cisterna (39°30'17.32"N, 8°36'55.06"W) is a fossil karst spring of the River Almonda (Zilhão 1997; Zilhão 2009). Its AMD2 locus, excavated 1988-89, featured an Early Neolithic funerary context contained in a shallow Holocene deposit that also yielded material related to later prehistoric uses of a similar nature. Even though the overwhelming majority of the ceramic assemblage, the stone tools and the body ornaments are Early Neolithic, the lack of unambiguous associations means that the age of the human remains could only be established by direct dating of individual specimens. Of those that returned results in the time range of the Cardial, two were successfully analyzed for ancient DNA: G21-631, a right M2 inserted in a mandible, and F19-385, a first phalanx from the right foot. The mandible was pretreated at the Max Planck Institute for Evolutionary Anthropology Department of Human Evolution, Leipzig (S-EVA 27412). Following the method described elsewhere (Talamo and Richards 2011)., the sample was graphitized and dated at the Curt-Engelhorn-Zentrum Archäometrie (Mannheim, Germany) (MAMS-18262) to 6,319±22 years BP (Table S1). The direct radiocarbon dating on the phalanx was done at ORAU (OxA-28855), which results in 6,280±34 years BP (Table S1).

Cova de l'Or

Cova de l'Or cave is a Cardial site located at the Sierra del Benicadell mountain range (Beniarrés, Alacant), 650 m above sea level (38°50'40.83"N, 0°21'50.83"W). Its entrance opens to the southwest, allowing natural light to illuminate its main chamber, which measures 24x8

metres (Martí Oliver 1977). The cave was first discovered in 1933. In 1955, Vicent Pascual and Julián San Valero directed several seasons of excavation under the auspices of the Servei d'Investigació Prehistòrica of the Diputació Provincial, in València. Decades later, between 1975 and 1985, excavations using modern techniques were done under the direction of Bernat Martí (Martí Oliver et al. 1980; Martí Oliver 1983). Several studies show that Cova de l'Or was first inhabited during the Early Neolithic, and was used as a place of habitation until the end of the Early Neolithic (ca. 4,800 years cal BCE), being later used as an animal pen (Badal García et al. 2012). Later on, in post-Neolithic times, it became a necropolis. The Cova de l'Or sample analysed for this study was removed from a human mandible belonging to a male adult individual excavated in 1957. Within the modern stratigraphic layout, it belongs to Level V, which dates to the end of the Cardial (Juan-Cabanilles 2008). The mandible was pretreated at the Max Planck Institute for Evolutionary Anthropology Department of Human Evolution, Leipzig (S-EVA 7649) and directly C^{14} dated at Mannheim (MAMS-19063), and yielded a date of 6,356±23 years BP (Table S1).

Cova de la Sarsa

Cova de la Sarsa is a Cardial site located in the northern slope of the Serra Mariola mountain range (Bocairent, València), 860 m above sea level (38°45'36.66"N, 0°34'56.70"W), having a total length of cave systems of 200 m. Although visited early on by Henri Breuil, Fernando Ponsell Cortés conducted the first excavations only in the 1920s. These excavations, funded by the Servei d'Investigació Prehistórica of Valencia, lasted until 1939. In the 1970's, María Dolores Asquerino Fernández excavated again the site (Asquerino Fernández 1978; Asquerino Fernández et al. 1998).

Despite the well-known importance of the site in the historiography of the western Mediterranean Neolithic, no precise stratigraphic sequence is currently available. Radiocarbon dating and pottery remains points to an intense inhabitation of the site during the Early Neolithic; more than 2,000 fragments of Cardial pottery have been found belonging to that period (García Borja et al. 2012). Two skeletons were discovered buried in a corridor leading from the main chamber to the inferior galleries, far from the living area (Casanova Vañó 1978), and associated to one Cardial vessel, three burins, a bone spoon, two bone rings, three C*olumbella* ornaments, one *Cardium* shell, three perforated *Pectunculus*, one fusiform bone object and some flint bladelets (García Borja et al. 2011).

These human remains correspond to female and male adults (García Borja et al. 2011). A female's vertebra sample was pretreated at the Max Planck Institute for Evolutionary Anthropology Department of Human Evolution, Leipzig (S-EVA 17064) and dated at ORAU (OxA-V-2392-26) to 6,341±30 years BP (Table S1). The sample analysed for this study is a second premolar of the male right maxilla recovered by V. Casanova. The sample was directly C14 dated at ORAU (OxA-31629), which resulted in 6,309±36 years BP (Table S1).

2- TMRCA estimate

TMRCA was inferred for the three available complete Early Neolithic genomes (Stuttgart, NE1 and CB13) using the program r8s (Sanderson 2003) and the Human Origins reference dataset. Positions with missing data in any of the three samples were excluded, resulting in a total of 276,901 genome-wide markers. To accurately calculate the distances between the samples, one allele at each position was randomly taken for NE1 and Stuttgart and then the number of changes between them and CB13 was computed 1000 times. Using the Langley-Fitch (LF) method with POWELL algorithm and fixing the terminal nodes to 7,200, 7,000 and 6,000 years BP for NE1, Stuttgart and CB13 respectively, resulted in an estimated TMRCA of 25,300 years BP. The obtained rate was 5.2e-06 substitutions per site per year; this

is much higher than the whole-genome rate but expected given that the included positions were selected for being polymorphic among extant populations.

Supplementary Figures

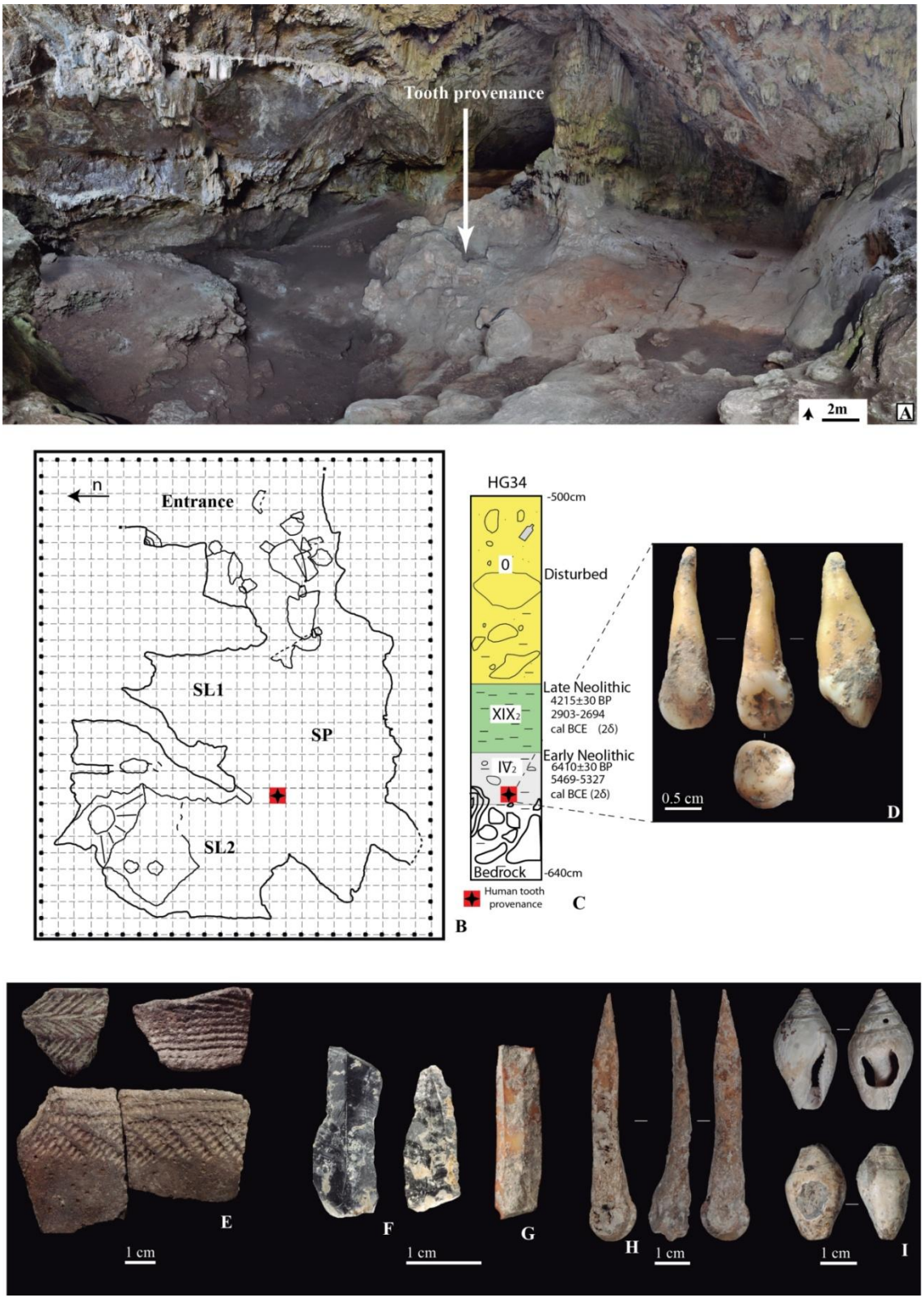

Fig. S1. Cova Bonica archaeological site and finds from the Cardial layer. (A) Panoramic view. (B) Site plan. (C) Stratigraphic column. (D) The CB13 upper canine tooth. (E) Cardial pottery. (F) Rock crystal bladelets. (G) Jasper bladelet. (H) Bone awl. (I) *Columbella rustica* ornaments.

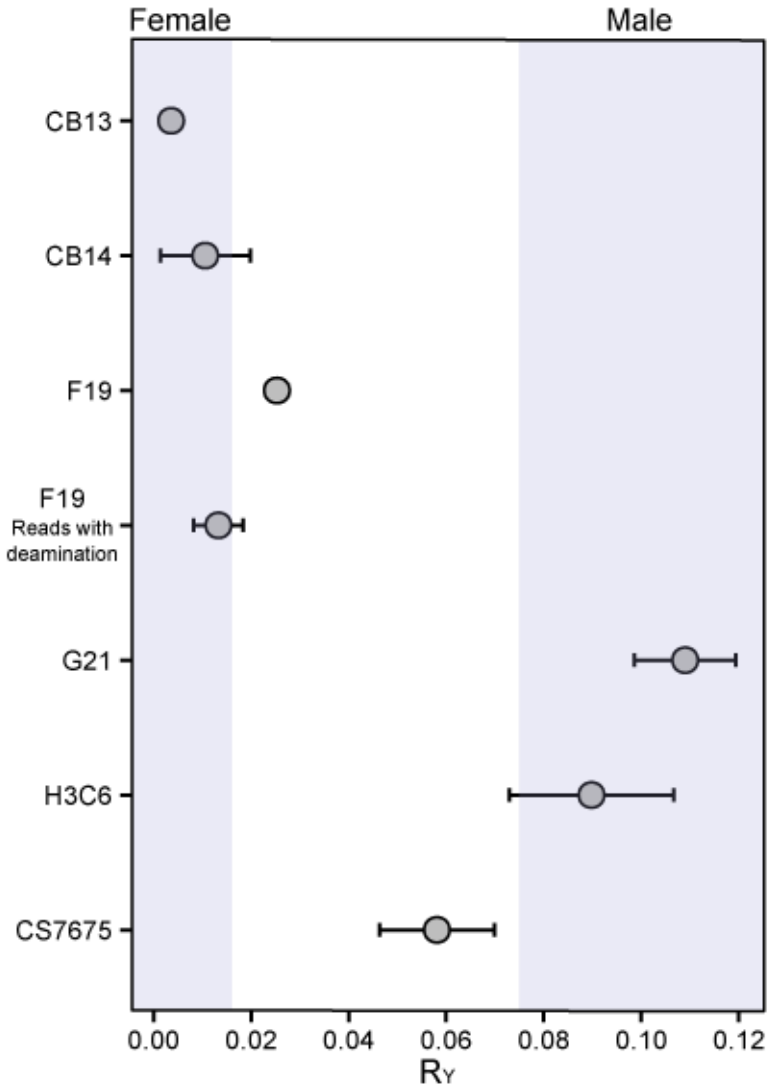

Fig. S2. Sex attribution for each Cardial sample based on the ratio of Y to X+Y chromosome reads, following Skoglund et al. (2013). The sample F19 is significantly contaminated; the analysis has been repeated including only the reads that show the typical ancient DNA deamination pattern at the end (PMDS > 4). The fact that it can be attributed to a female with higher probability suggests that the contaminant individual is a male.

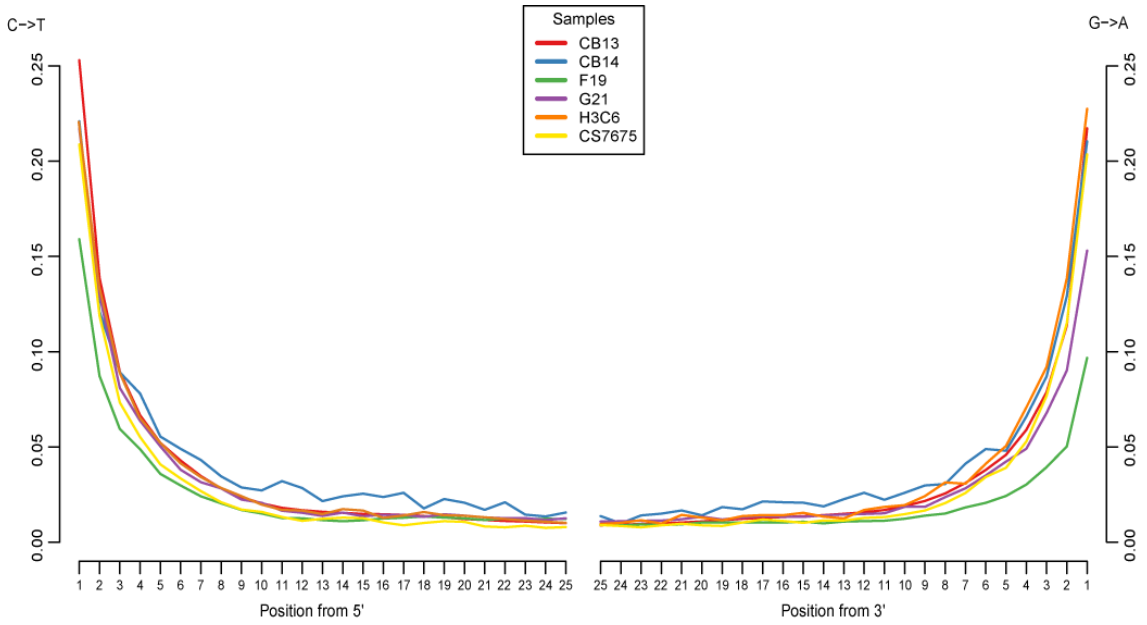

Fig. S3. Misincorporation pattern at the ends of the reads of the Cardial samples. On the left, C to T deamination rate at the 5' end. On the right, G to A deamination rate at the 3' end. Figures around or over 20% are compatible with the values obtained for other Neolithic samples. Deamination rates for F19 are lower due to the presence of significant levels of modern contamination in this specimen.

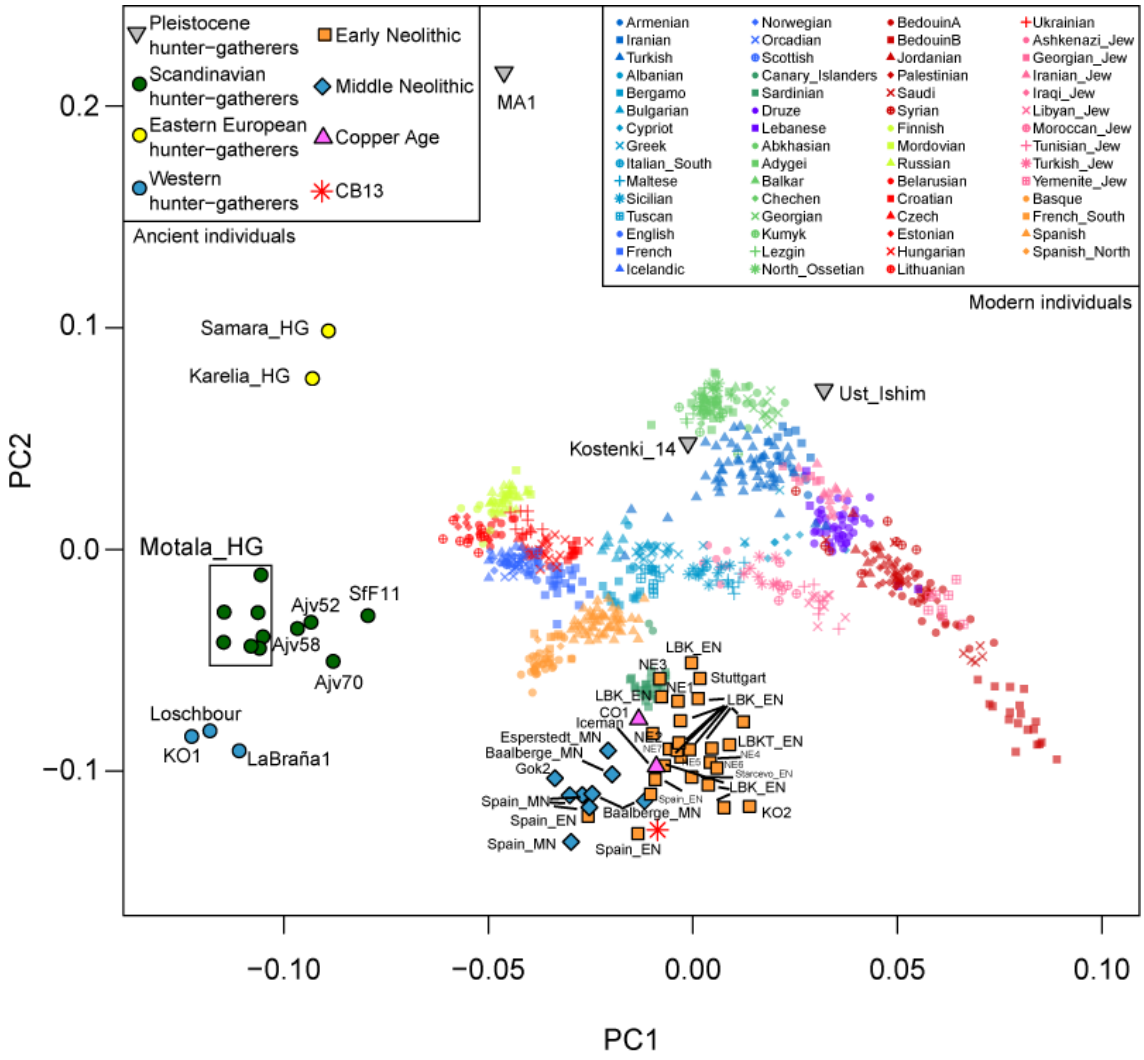

Fig. S4. Procrustes PCA using only transversion sites and including ancient genomes (from the Pleistocene up to the Cooper Age) and modern West Eurasians. Complement of Figure 2A with identification labels.

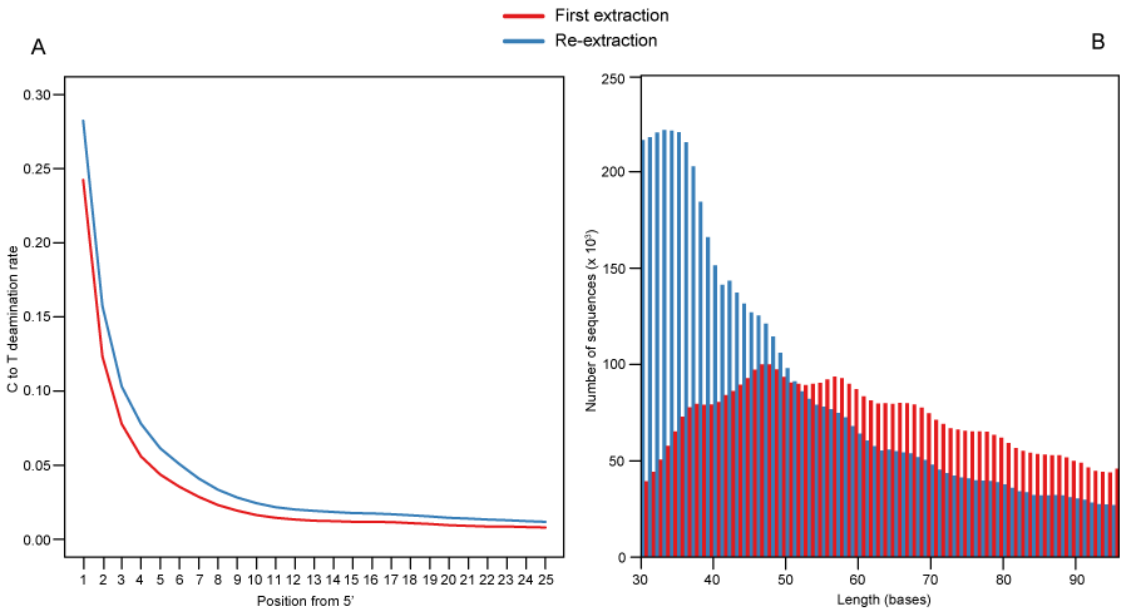

Fig. S5. Comparison between CB13 DNA libraries constructed from the first extract (red) and from the reextraction (blue). (A) Frequency of C to T misincorporations at the 5' end of the reads. (B) Fragment length distribution of reads mapping to the nuclear genome. The DNA library constructed from the re-extraction yielded shorter DNA fragments with higher deamination rate than the previous libraries.

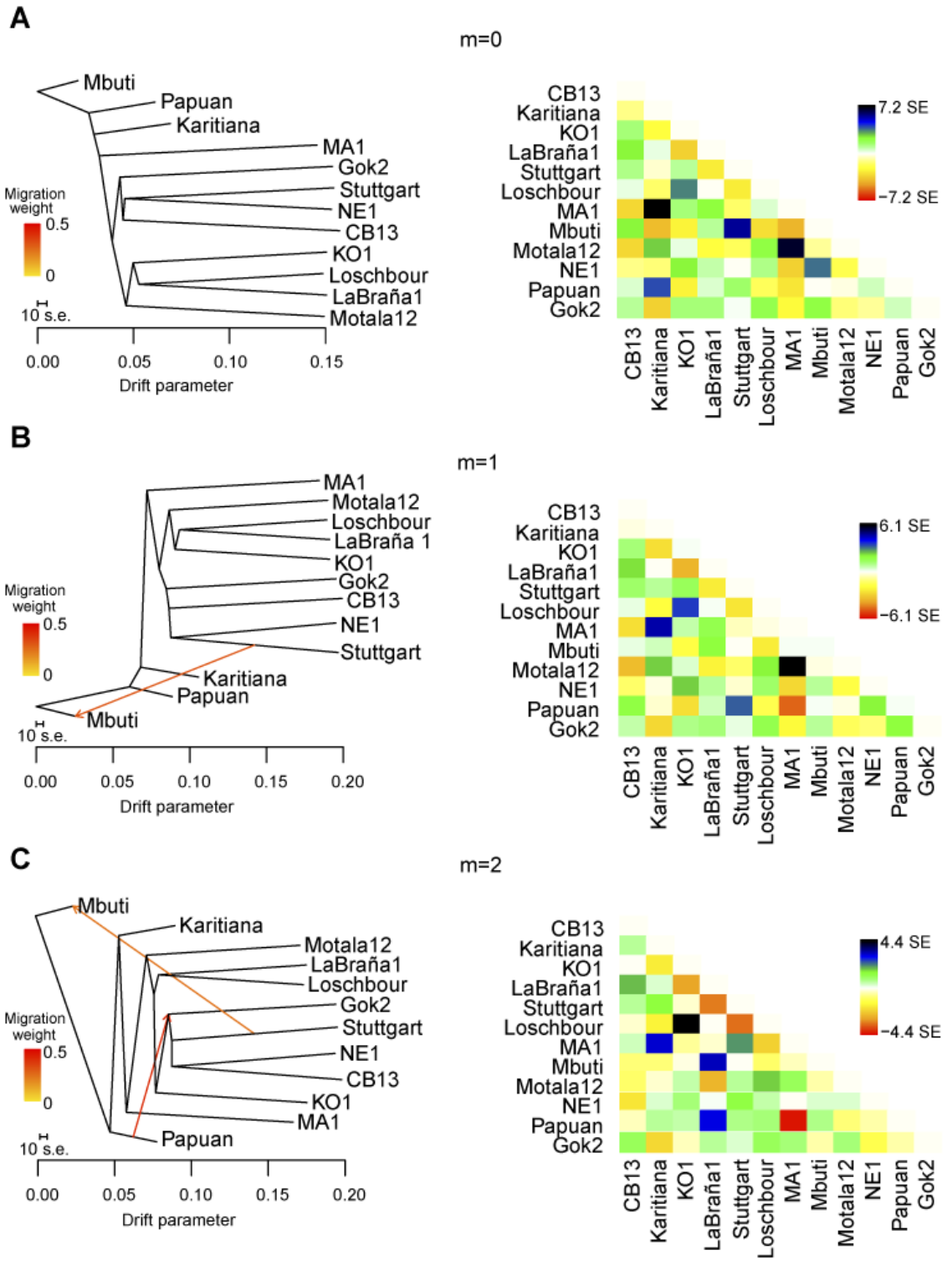

Fig. S6. *TreeMix* (Pickrell and Pritchard 2012) analysis considering: (A) no migration edges, (B) one migration edge and (C) two migration edges.

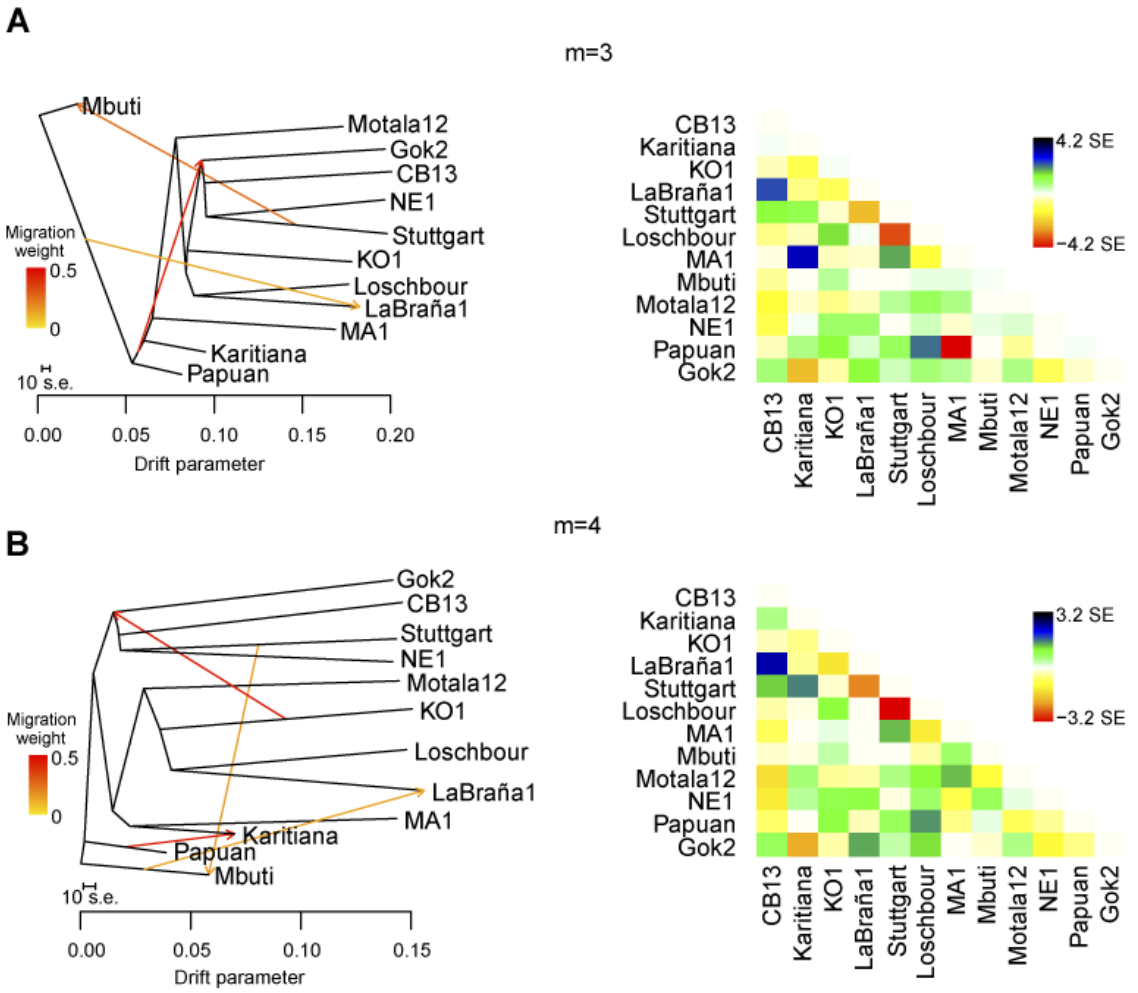

Fig. S7. *TreeMix* (Pickrell and Pritchard 2012) analysis considering: (A) three migration edges and (B) four migration edges.

Supplementary Tables

Table S1. AMS radiocarbon dating for all the sites mentioned in the paper. Calibrated using Oxcal 4.2 (Bronk Ramsey and Lee 2013) with the Intcal13 curve (Reimer et al. 2013).

Site	Layer	Sample Code	Species	Anatomical part	MPI Code	AMS Nr	^{14}C Age	1σ Err	Cal BCE 1σ		Cal BCE 2σ	
									From	*to*	*From*	*to*
Cova Bonica	IV_2	CB13-HH34-IV_2-2407	Human	Upper canine		Beta-384724	6410	30	5470	5360	5470	5320
Galeria da Cisterna	-	G21-631	Human	Mandible	S-EVA 27412	MAMS-18262	6319	22	5330	5230	5360	5220
Galeria da Cisterna	-	F19-385	Human	First phalanx		OxA-28855	6280	34	5310	5220	5330	5200
Cova de l'Or	V	-	Human	Mandible	S-EVA 7649	MAMS-19063	6356	23	5360	5310	5470	5290
Cova de la Sarsa[a]	-	-	Human	Second premolar		OxA-31629	6309	36	5321	5227	5360	5217
Cova de la Sarsa	-	-	Human	Vertebra	S-EVA 17064	OxA-V-2392-26	6341	30	5370	5300	5470	5220

[a] Sample analysed in this study

Table S2. Statistics for the different samples and libraries sequenced in this study (SHOT: shotgun; CAP: whole genome capture).

Library	Raw reads	Mapped reads	Human DNA (%)	Unique reads	Mean read length
CB13_46_SHOT	497,224,346	21,566,750	4.34	6,526,834	73.46
CB13_14_SHOT	400,658,464	23,004,860	5.74	6,795,635	74.84
CB13_18_SHOT	209,074,549	9,231,631	4.42	867,163	73.53
CB13_19_SHOT	202,044,458	8,600,972	4.26	845,573	73.43
CB13_20_SHOT	163,338,533	7,032,874	4.31	720,476	73.52
CB13_15_SHOT (reextraction)	1,050,188,254	73,933,019	7.04	28,376,568	61.74
CB13_7_CAP	441,785,724	124,731,162	28.23	2,626,830	81.11
CB14_33_SHOT	28,563,379	71,874	0.25	14,688	65.43
F19_SHOT	15,466,637	90,441	0.58	89,316	78.87
F19_2_CAP	39,679,389	3,831,422	9.66	391,383	89.27
G21_SHOT	21,143,726	18,565	0.09	18,128	74.34
G21_1_CAP	60,298,287	768,465	1.27	141,799	84.55
H3C6_SHOT	22,620,364	13,513	0.06	12,286	49.97
H3C6_9_CAP	44,454,074	447,838	1.01	46,031	61.85
CS7675_29_SHOT	199,059,953	149,550	0.08	41,717	55.75
CS7675_3_CAP	55,715,268	637,629	1.14	20,064	68.47

Table S3. Contamination estimates at the mtDNA genome following the Bayesian method of Fu et al. (2013). Due to the low coverage, it was not possible to estimate contamination for CS7675 sample.

Sample	MtDNA coverage	MtDNA reads MQ>30	Contamination estimate (%)	Lower CI limit (%)	Upper CI limit (%)
CB13	353.29	63,415	0.11	0.02	2.34
CB14	4.1	975	1.35	0.22	15.76
F19	33.79	6,581	29.13	25.53	33.01
G21	63.55	13,553	1.97	0.76	3.74
H3C6	4.45	1,303	3.96	0.96	12.24
CS7675	0.69	224	-	-	-

Table S4. CB13 mitochondrial DNA contamination estimates by assessing the nucleotide substitutions present at the K1a2a haplotype diagnostic positions.

Position	rCRS	CB13	Haplogroup	CB13 / Total	Contamination %
11467	A	G	U	286/305	6.23
12308	A	G	U	332/346	4.05
12372	G	A	U	297/297	0
1811	A	G	U2'3'4'7'8'9	297/314	5.41
9698	T	C	U8	316/334	5.39
3480	A	G	U8b'c	301/319	5.64
9055	G	A	U8b	312/315	0.96
14167	C	T	U8b	307/307	0
10550	A	G	K	265/275	3.64
11299	T	C	K	297/314	5.41
14798	T	C	K	306/320	4.38
16224	T	C	K	271/282	3.90
16311	T	C	K	271/281	3.56
1189	T	C	K1	300/323	7.12
10398	A	G	K1	313/330	5.15
497	C	T	K1a	264/264	0
11025	T	C	K1a2	278/292	4.79
5773	G	A	K1a2a	372/376	1.06
			Total	5,385/5,594	3.74 (3.23 - 4.23, 95% C.I.)
			Total[a]	1,552/1,559	0.45 (0.12 – 0.78, 95% C.I.)

[a]Excluding positions affected by post-mortem DNA damage

Table S5. Mitochondrial DNA haplogroup attribution of the Cardial samples.

Sample ID	Haplogroup	HaploGrep's Quality	Polymorphisms	Coverage
CB13	K1a2a	99.3	73G, 263G, 497T, 750G, 1189C, 1438G, 1811G, 2706G, 3480G, 4769G, 5773A, 7028T, 8860G, 9055A, 9698C, 10398G, 10550G, 11025C, 11299C, 11467G, 11719A, 12308G, 12372A, 14167T, 14766T, 14798C, 15326G, 16224C, 16311C, 16519C	353.29
CB14	X2c	76.0	73G, 153G, 195C, 225A, 227G, 263G, 750G,1719A, 2706G, 4769G, 6371T, 7028T, 8860G, 11719A, 12705T, 13966G, 14766T, 15326G, 16189C, 16223T, 16255A, 16278T	4.1
F19	H4a1a	100	263G, 750G, 1438G, 3992T, 4024G, 4769G, 5004C, 8269A, 8860G, 9123A, 14365T, 14582G, 15326G	33.79
G21	H3	100	263G, 750G, 1438G, 4769G, 6776C, 8860G, 15326G, 16519C	63.55
H3C6	H4a1a	86.6	263G, 750G, 1438G, 3992T, 4024G, 5004C, 8269A, 8860G, 14365T, 14582G, 15326G	4.45
CS7675	K1a4a1	53.2	263G, 497T, 750G, 1811G, 3480G, 7028T, 11719A, 11840T, 12372A, 13740C, 14766T, 14798C	0.69

Positions in red are represented by less than 3 reads

Table S6. Cova Bonica CB13 alleles for the SNPs included in the 8-plex pigmentation phenotype prediction.

ID	Gene	Ancestral	Derived	Genotype
rs12913832	*OCA2-HERC2*	A	G	No data
rs1545397	*OCA2*	A	T	A (2x)
rs16891982	*SLC45A2*	C	G	2C,1G (3x)
rs885479	*MC1R*	G	A	G (5x)
rs1426654	*SLC24A5*	G	A	A (2x)
rs12896399	*SLC24A4*	G	T	G (1x)
rs6119471	*ASIP*	G	C	C (1x)
rs12203592	*IRF4*	C	T	C (1x)

Table S7. Cova Bonica CB13 alleles for the SNPs included in the Hirisplex pigmentation phenotype prediction.

ID	Gene	Ancestral	Derived	Genotype
N29insA	*MC1R*	C	A	C (2x)
rs11547464	*MC1R*	G	A	G (5x)
rs885479	*MC1R*	G	A	G (5x)
rs1805008	*MC1R*	C	T	C (6x)
rs1805005	*MC1R*	G	T	G (1x)
rs1805006	*MC1R*	C	A	No data
rs1805007	*MC1R*	C	T	C (3x)
rs1805009	*MC1R*	G	C	G (1x)
Y152OCH	*MC1R*	C	A	C (3x)
rs2228479	*MC1R*	G	A	G (2x)
rs1110400	*MC1R*	T	C	T (3x)
rs28777	*SLC45A2*	C	A	No data
rs16891982	*SLC45A2*	C	G	2C,1G (3x)
rs12821256	*KITLG*	T	C	T (5x)
rs4959270	*EXOC2*	C	A	C (1x)
rs12203592	*IRF4*	C	T	C (1x)
rs1042602	*TYR*	C	A	A (1x)
rs1800407	*OCA2*	C	T	No data
rs2402130	*SLC24A4*	G	A	A (1x)
rs12913832	*OCA2-HERC2*	A	G	No data
rs2378249	*ASIP/PIGU*	A	G	No data
rs12896399	*SLC24A4*	G	T	G (1x)
rs1393350	*TYR*	G	A	G (2x)
rs683	*TYRP1*	A	C	No data

Table S8. Cova Bonica CB13 alleles at the SLC24A5 region to ascertain the haplotype around the light skin allele.

ID	Gene	Ancestral	Derived	Genotype
rs1834640	*SLC24A5*	G	A	No data
rs2675345	*SLC24A5*	G	A	A (1x)
rs2469592	*SLC24A5*	G	A	A (2x)
rs2470101	*SLC24A5*	C	T	T (1x)
rs938505	*SLC24A5*	C	T	No data
rs2433354	*SLC24A5*	T	C	No data
rs2459391	*SLC24A5*	G	A	No data
rs2433356	*SLC24A5*	A	G	No data
rs2675347	*SLC24A5*	G	A	A (2x)
rs2675348	*SLC24A5*	G	A	A (1x)
rs1426654	*SLC24A5*	G	A	A (2x)
rs2470102	*SLC24A5*	G	A	No data
rs16960631	*SLC24A5*	A	G	A (1x)
rs2675349	*SLC24A5*	G	A	A (2x)
rs3817315	*SLC24A5*	T	C	No data
rs7163587	*SLC24A5*	T	C	No data

Table S9. Cova Bonica CB13 alleles at the OCA2/HERC2 region to ascertain the haplotype around the blue-eyes mutation.

ID	Gene	Ancestral	Derived	Genotype
rs4778241	*OCA2-HERC2*	A	C	C (1x)
rs1129038	*OCA2-HERC2*	C	T	1C,2T (3x)
rs12593929	*OCA2-HERC2*	G	A	A (1x)
rs12913832	*OCA2-HERC2*	A	G	No data
rs7183877	*OCA2-HERC2*	C	A	C (2x)
rs3935591	*OCA2-HERC2*	T	C	C (3x)
rs7170852	*OCA2-HERC2*	T	A	A (2x)
rs2238289	*OCA2-HERC2*	A	G	A (2x)
rs3940272	*OCA2-HERC2*	T	G	G (1x)
rs8028689	*OCA2-HERC2*	C	T	No data
rs2240203	*OCA2-HERC2*	C	T	T (1x)
rs11631797	*OCA2-HERC2*	A	G	No data
rs916977	*OCA2-HERC2*	T	C	No data

Table S10. D-stat of the form D (HG1, HG2, Neolithic Farmer, Outgroup). Standard errors (SE) were computed using block jackknife over 5Mb blocks.

HG1	HG2	Neolithic Farmer	D-stat	SE	Z	D-stat (only transversions)	SE	Z
KO1	LaBraña1	CB13	0.0229	0.0053405	4.288	0.0252	0.0055494	4.541
KO1	LaBraña1	Stuttgart	0.0251	0.0054435	4.611	0.0241	0.0059536	4.048
KO1	LaBraña1	NE1	0.0253	0.0057868	4.372	0.029	0.0063806	4.545
KO1	LaBraña1	Gok2	0.0178	0.0052725	3.376	0.0215	0.0059922	3.588
Loschbour	LaBraña1	CB13	0.0062	0.0067983	0.912	0.0073	0.0069923	1.044
Loschbour	LaBraña1	Stuttgart	0.013	0.0057345	2.267	0.0118	0.0062236	1.896
Loschbour	LaBraña1	NE1	0.0047	0.0050756	0.926	0.0039	0.005644	0.691
Loschbour	LaBraña1	Gok2	0.0116	0.0050833	2.282	0.0193	0.0058895	3.277
KO1	Loschbour	CB13	0.0172	0.0068471	2.512	0.0179	0.0072823	2.458
KO1	Loschbour	Stuttgart	0.0111	0.0063757	1.741	0.0097	0.0068022	1.426
KO1	Loschbour	NE1	0.0193	0.0049335	3.912	0.021	0.0050909	4.125
KO1	Loschbour	Gok2	0.0062	0.0049363	1.256	0.0015	0.0060729	0.247
KO1	Motala12	CB13	0.0226	0.0060074	3.762	0.0222	0.0064516	3.441
KO1	Motala12	Stuttgart	0.0116	0.0055609	2.086	0.0102	0.006387	1.597
KO1	Motala12	NE1	0.0263	0.0053849	4.884	0.0242	0.0060758	3.983
KO1	Motala12	Gok2	0.0222	0.0063738	3.483	0.0158	0.0067928	2.326
LaBraña1	Motala12	CB13	0.0011	0.0052632	0.209	-0.0019	0.0055719	-0.341
LaBraña1	Motala12	Stuttgart	-0.0118	0.0056513	-2.088	-0.0103	0.0061677	-1.67
LaBraña1	Motala12	NE1	0.0024	0.0048387	0.496	-0.0003	0.0042857	-0.07
LaBraña1	Motala12	Gok2	0.005	0.0056689	0.882	-0.0033	0.0062857	-0.525
Loschbour	Motala12	CB13	0.0073	0.007026	1.039	0.0065	0.0071272	0.912
Loschbour	Motala12	Stuttgart	0.0011	0.0061453	0.179	0.0018	0.0064516	0.279
Loschbour	Motala12	NE1	0.0075	0.0047111	1.592	0.0033	0.0054098	0.61
Loschbour	Motala12	Gok2	0.0175	0.0060366	2.899	0.0176	0.0062925	2.797

References

Asquerino Fernández MD, López P, Molero G, Sevilla P, Aparicio MT, Ramos M. 1998. Cova de la Sarsa (Bocairent, Valencia). Sector II: Gatera. *Recerques del Museu d'Alcoi* 7:47–88.

Asquerino Fernández MD. 1978. Cova de la Sarsa (Bocairente, Valencia). Análisis estadístico y tipológico de materiales sin estratigrafía (1971-1974). *Sagvntvm. Papeles del laboratorio de Arqueología de Valencia* 13:99–225.

Badal García E, Martí Oliver B, Pérez-Ripoll M. 2012. From agricultural to pastoral use: changes in neolithic landscape at Cova de l'Or (Alicante, Spain). In: Wood and charcoal. Evidence for human and natural history. Sagvntvm Extra-13. p. 75–84.

Bronk Ramsey C, Lee S. 2013. Recent and planned developments of the program oxcal. *Radiocarbon* 55:720–730.

Casanova Vañó V. 1978. Enterramiento doble en la Cova de la Sarsa (Bocairent, València). *Archivo de Prehistoria Levantina* 15:27–36.

Fu Q, Mittnik A, Johnson PLF, Bos K, Lari M, Bollongino R, Sun C, Giemsch L, Schmitz R, Burger J, et al. 2013. A revised timescale for human evolution based on ancient mitochondrial genomes. *Curr. Biol.* 23:553–559.

García Borja P, Salazar-García D, Martins H, Pérez Jordà G, Sanchis Serra A. 2012. Dataciones radiocarbónicas de la Cova de la Sarsa (Bocairent, València). *Recerques del Museu d'Alcoi* 22:19–24.

García Borja P, Salazar-García DC, Pérez Fernández A, Pardo Gordó S, Casanova Vañó V. 2011. El Neolítico antiguo cardial y la Cova de la Sarsa (Bocairent, València). Nuevas perspectivas a partir de su registro funerario. *Munibe. Arqueología Antropología*. 62:175–195.

Juan-Cabanilles J. 2008. El utillaje de piedra tallada en la Prehistoria reciente valenciana. Aspectos tipológicos, estilísticos y evolutivos. Serie de Trabajos Varios del Servicio de Investigación Prehistórica de la Diputación Provincial de Valencia

Martí Oliver B, Pascual Pérez V, Gallart Martí D, López García P, Pérez Ripoll M, Acuña Hernández JD, Robles Cuenca F. 1980. Cova de l'Or (Beniarrés Alicante) Vol. II. Serie de Trabajos Varios del Servicio de Investigación Prehistórica de la Diputación Provincial de Valencia

Martí Oliver B. 1977. Cova de l'Or (Beniarrés Alicante) Vol. I. Valencia: Serie de Trabajos Varios del Servicio de Investigación Prehistórica de la Diputación Provincial de Valencia

Martí Oliver B. 1983. Cova de l'Or (Beniarrés, Alicante). Memorias de las campañas de excavación 1975-1979. *Noticiario Arqueológico Hispánico* 16:11–55.

Pickrell JK, Pritchard JK. 2012. Inference of population splits and mixtures from genome-wide allele frequency data. PLoS Genet. 8:e1002967.

Reimer PJ, Bard E, Bayliss A, Beck JW, Blackwell PG, Bronk C, Caitlin R, Hai EB, Edwards RL. 2013. Intcal13 and marine13 radiocarbon age calibration curves 0 – 50,000 years cal bp. *Radiocarbon* 55:1869–1887.

Sanderson MJ. 2003. r8s: inferring absolute rates of molecular evolution and divergence times in the absence of a molecular clock. Bioinformatics 19:301–302.

Skoglund P, Storå J, Götherström A, Jakobsson M. 2013. Accurate sex identification of ancient human remains using DNA shotgun sequencing. *J. Archaeol. Sci.* 40:4477–4482.

Talamo S, Richards M. 2011. A comparison of bone pretreatment methods for AMS dating of samples >30,000 BP. *Radiocarbon* 53:443–449.

Zilhão J. 1997. O Paleolítico Superior da Estremadura portuguesa. Lisboa: Colibri

Zilhão J. 2009. The Early Neolithic artifact assemblage from the Galeria da Cisterna (Almonda karstic system, Torres Novas, Portugal). In: De Méditerranée et d'ailleurs. Mélanges offerts à Jean Guilaine. Toulouse: Archives d'Écologie Préhistorique. p. 821–835.